

Electrical conduction of LiF interlayers in organic diodes

Cite as: J. Appl. Phys. **117**, 155502 (2015); <https://doi.org/10.1063/1.4917461>

Submitted: 14 January 2015 . Accepted: 01 April 2015 . Published Online: 16 April 2015

Benjamin F. Bory, Henrique L. Gomes, René A. J. Janssen, Dago M. de Leeuw, and Stefan C. J. Meskers



View Online



Export Citation



CrossMark

ARTICLES YOU MAY BE INTERESTED IN

[Lithium fluoride injection layers can form quasi-Ohmic contacts for both holes and electrons](#)
Applied Physics Letters **105**, 123302 (2014); <https://doi.org/10.1063/1.4896636>

[Enhanced electron injection in organic electroluminescence devices using an Al/LiF electrode](#)
Applied Physics Letters **70**, 152 (1997); <https://doi.org/10.1063/1.118344>

[Organic electroluminescent diodes](#)
Applied Physics Letters **51**, 913 (1987); <https://doi.org/10.1063/1.98799>

Ultra High Performance SDD Detectors



See all our XRF Solutions

Electrical conduction of LiF interlayers in organic diodes

Benjamin F. Bory,¹ Henrique L. Gomes,² René A. J. Janssen,¹ Dago M. de Leeuw,³ and Stefan C. J. Meskers^{1,a)}

¹Molecular Materials and Nanosystems and Institute for Complex Molecular Systems, Eindhoven University of Technology, P.O. Box 513, 5600 MB Eindhoven, The Netherlands

²Instituto de Telecomunicações, Av. Rovisco Pais, 1, 1049-001, Lisboa, Portugal and Universidade do Algarve, Campus de Gambelas, 8005-139 Faro, Portugal

³Max-Planck Institute for Polymer Research, Ackermannweg 10, 55128 Mainz, Germany and King Abdulaziz University, Jeddah, Saudi Arabia

(Received 14 January 2015; accepted 1 April 2015; published online 16 April 2015)

An interlayer of LiF in between a metal and an organic semiconductor is commonly used to improve the electron injection. Here, we investigate the effect of moderate bias voltages on the electrical properties of Al/LiF/poly(spirofluorene)/Ba/Al diodes by systematically varying the thickness of the LiF layer (2–50 nm). Application of forward bias V below the bandgap of LiF ($V < E_g \sim 14$ V) results in reversible formation of an electrical double layer at the LiF/poly(spirofluorene) hetero-junction. Electrons are trapped on the poly(spirofluorene) side of the junction, while positively charged defects accumulate in the LiF with number densities as high as $10^{25}/\text{m}^3$. Optoelectronic measurements confirm the built-up of aggregated, ionized F centres in the LiF as the positive trapped charges. The charged defects result in efficient transport of electrons from the polymer across the LiF, with current densities that are practically independent of the thickness of the LiF layer. © 2015 Author(s). All article content, except where otherwise noted, is licensed under a Creative Commons Attribution 3.0 Unported License.

[<http://dx.doi.org/10.1063/1.4917461>]

I. INTRODUCTION

Among the inorganic semiconductors, lithium fluoride has the largest bandgap (~ 14 eV (Ref. 1)) and the largest known negative electron affinity (-3 eV (Ref. 2)). Surprisingly, despite its seemingly inaccessible conduction band, LiF is widely used in light emitting diodes as interlayer between organic semiconductors and metals to improve electron injection.^{3,4} In addition, in organic solar cells, thin LiF layers are commonly used to improve electron extraction.⁵

A thin layer of LiF (1–3 nm) on a metal electrode is known to change the effective work function of the electrode.^{6,7} The mechanism by which this change in work function occurs is still under debate.^{8–10} A thin LiF layer on a metal electrode lowers the work function of the electrode.

Thicker layers of LiF (5–50 nm) show more complex behaviour. In their pristine state, these layers are too thick to transport charge carriers via tunnelling and the LiF layer behaves as an insulator. However, the electrical transport properties dramatically change when for a prolonged time a bias voltage is applied. Here, we investigate in detail the early stages of this electroforming process for LiF layers with a thickness exceeding 10 nm. The structure of the diodes under investigation is schematically depicted in Fig. 1(a). The diodes contain a bilayer of LiF and an organic semiconductor, poly(spirofluorene). Application of moderate bias voltage stress with potential differences smaller than the band gap results in accumulation of trapped positive charge in the LiF layer. The charges accumulate slowly, on the time

scale of seconds. In turn, the trapped positive charges induce an efficient transport of electrons from the organic semiconductor through the LiF layer into the metal electrode.

The electroforming process is schematically depicted in Fig. 1. The flat band diagram of the pristine diode is shown

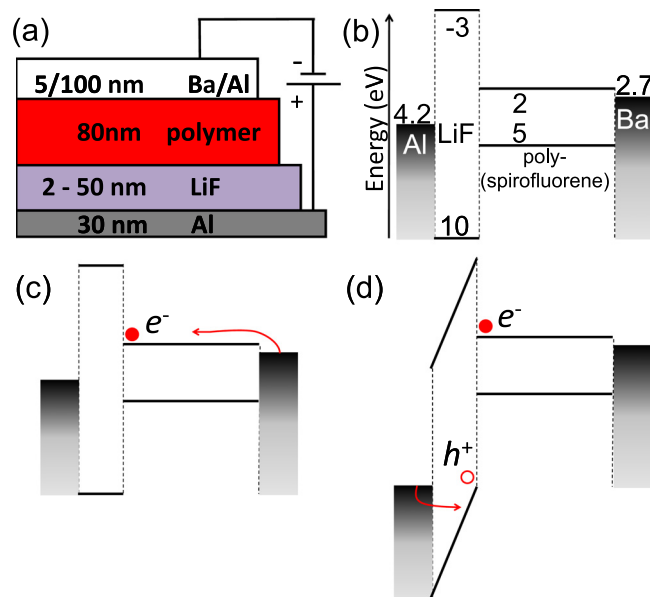


FIG. 1. (a) Diode structure Al/LiF/poly(spirofluorene)/Ba/Al. (b) Flat band diagram illustrating the valence and conduction bands of poly(spirofluorene) and LiF^{2,11} and the work functions of Al and Ba with respect to the vacuum level, before exchange of charge between the materials. (c) Electron injection under low forward bias and (d) hole injection into LiF under moderate forward bias and trapping, resulting in a charge transfer state.

^{a)}Email: s.c.j.meskers@tue.nl

in Fig. 1(b). The poly(spirofluorene)/Ba/Al top contact has quasi-ohmic properties for injection of electrons.¹² Upon biasing the top Ba/Al electrode negative with respect to the bottom Al electrode, with a voltage exceeding the built-in voltage of about 1.5 V, *viz.*, the difference between the work function of the bottom Al and the top Ba/Al electrode, we expect injection of electrons into the polymeric semiconductor (Fig. 1(c)). The LiF/poly(spirofluorene) bilayer constitutes a hetero-junction. Specific interface related electronic states may be populated by applying a medium bias voltage below the bandgap of the alkali halide. One of these interface states is illustrated in Fig. 1(d) and involves a negative charge on the organic semiconductor and a positive charge in the LiF.

Because the LiF is a material with negative electron affinity, a surface bound, charge transfer state exists at the LiF-vacuum interface, which has been detected experimentally at energies above 9.7 eV.¹³ Now considering the LiF/poly(spirofluorene) hetero-junction and taking into account that the lowest unoccupied electron level in the semiconducting polymer is roughly 2 eV below the vacuum level, it follows that population of the charge transfer configuration should be allowed energetically for bias voltages of 8 V. Coulombic interactions between positive and negative charges and (self-) trapping of the positive charges in the LiF will further lower the voltage required for accumulation of a dipolar charge distribution across the LiF/polymer interface, consistent with the intermediate voltages applied in this study.

LiF, and alkali halides in general, are known to be very susceptible to radiation damage. Irradiation with quanta of energy exceeding the bandgap leads to defect formation with considerable efficiency. Excitons in LiF are unstable and undergo self-trapping that can lead to defect formation.¹⁴ This is usually rationalized by the energy for formation of Frenkel defects, consisting of an anion vacancy and a corresponding halide interstitial, actually being lower than the bandgap of the alkali halide,¹⁵ so that electronic excitation of the alkali halide can result in defect formation with high yield.

Here we focus on the very early stages of electroforming of the complex electroforming process. We avoid extensive defect formation associated with application of bias voltages close to the bandgap, by restricting the bias voltage to ≤ 15 V. Our hypothesis is that upon applying such intermediate bias voltages, a charge double layer should form at the LiF/poly(spirofluorene) interface, as illustrated in Fig. 1(d). We note that for Al₂O₃/polymer diodes experimental evidence for such double layer formation exists.¹⁶

The detailed studies presented here into the very early stages of the electroforming are motivated by the need to understand the electrical stability of LiF interface layers in organic electronics and the prospect of non-volatile electronic data storage in electroformed diodes as possible replacement of NAND-flash circuitry.¹⁷

The organization of this paper is as follows. After describing the experimental details, we first investigate the LiF/poly(spirofluorene) hetero-junction using dc and ac electrical methods. The thickness of the LiF layer is varied systematically. We then employ electro-optical methods to find

further evidence for accumulation of charges near the LiF/poly(spirofluorene) interface and estimate the doping density in the LiF layers.

II. MATERIALS AND METHODS

Diodes with an Al/LiF/poly(spirofluorene)/Ba/Al layout as shown in Fig. 1(a) were fabricated under clean room conditions on glass wafers. The Al bottom electrode was deposited by vacuum sublimation using a patterned mask. The LiF was deposited by thermal sublimation under high vacuum onto the entire substrate area. The layer of poly(spirofluorene) semiconducting polymer (CB01, Covion) was spin cast in air from toluene. The top Ba/Al top electrode was thermally sublimated under vacuum through a shadow mask. All the diodes were encapsulated with stainless steel caps glued onto the substrate. At the site where the glue is applied, the semiconducting polymer was removed by laser ablation to avoid the diffusion of water through the polymer. A getter was placed into the stainless steel cap to exclude water. The encapsulated diodes have active areas of 1 or 9 mm². Due to the encapsulation, the devices are stable for years. For reference measurements also, similar diodes with Al/Al₂O₃/poly(spirofluorene)/Ba/Al layout were fabricated using RF sputtering to deposit the oxide.

To separately characterize the electron transport through the polymer, electron-only diodes with an Al/poly(spirofluorene)/Ba/Al structure, including a thin native oxide layer on the bottom electrode, were fabricated as follows. The bottom electrode, consisting of patterned vapor deposited Al on glass, was oxidized in air. On top, a thin layer of poly(spirofluorene) was spin cast from toluene in a glove box.¹² The top Ba/Al contact was thermally sublimated under vacuum through a shadow mask.

For opto-electronic measurements, ITO/LiF/poly(spirofluorene)/Ba/Al diodes were fabricated by thermal sublimation of LiF under 10⁻⁶ mbar directly onto glass substrates with patterned ITO. ITO substrates were cleaned, using in order, acetone, soap scrubbing and isopropanol. The poly(spirofluorene) was dissolved in toluene at a concentration of 5 mg/ml and spin-coated at a speed of 630 rpm. Subsequently, Ba and Al were deposited by thermal sublimation under vacuum. Diodes on ITO substrates were not encapsulated but kept under inert atmosphere (N₂, O₂, H₂O < 1 ppm) at all times during fabrication and characterization.

Current density-voltage characteristics were obtained using an Agilent semiconductor parameter analyzer 4155C. Throughout this study, positive (forward) bias is defined as the Ba/Al top electrode being negative. Small-signal impedance spectroscopy was performed with a Solartron 1260 impedance analyzer. The conductance G_p was obtained from the real part of the admittance and the loss was calculated as G_p/ω with ω the radial frequency. The parallel capacitance C_p was obtained from the imaginary component of the admittance (or susceptance B_p) by taking B_p/ω . Reflection experiments were performed using a Perkin Elmer λ 900 UV-Vis-NIR absorbance spectrometer with a module for specular reflection measurements.

III. ELECTRICAL CHARACTERIZATION

Pristine Al/alkali halide/poly(spirofluorene)/Ba/Al diodes were submitted to sequential cyclic current-voltage (J - V) scans with the bias starting at 0 V, going to a maximum and then back to zero bias, see Fig. 2(a). For negative bias voltages, very low current densities are observed that are consistent with the displacement current expected for the LiF/poly(spirofluorene) dielectric. For positive bias voltage, the current densities are much higher and the diode shows considerable rectification. For positive bias voltages, the current measured depends on the history of the diode. In the first scan from 0 V \rightarrow +2 V \rightarrow 0 V, we observe hysteresis. Moreover, in the second scan from 0 V \rightarrow +4 V \rightarrow 0 V the current density in the voltage range 0 V \rightarrow +2 V is much lower than in the first sweep up to +2 V. Interestingly, when the bias voltage is swept of the range +2 V \rightarrow +4 V, the current density is high again. The curve continues the first 0 V \rightarrow +2 V sweep. Similar history dependent features and hysteresis have been observed for Al/Al₂O₃/poly(spirofluorene)/Ba/Al diodes.¹⁸ The hysteresis can be interpreted in terms of trapping of electrons at the LiF/polymer interface.

The trapping of electrons is confirmed by quasi-static capacitance voltage (QSCV) measurements, see Fig. 2(b). The voltage-step QSCV method is very well suited to investigate traps that fill quickly but empty slowly.^{19,20} The method involves stepping the applied bias with 0.1 V increment and determining the capacitance via integration of the transient displacement current after each bias increment.

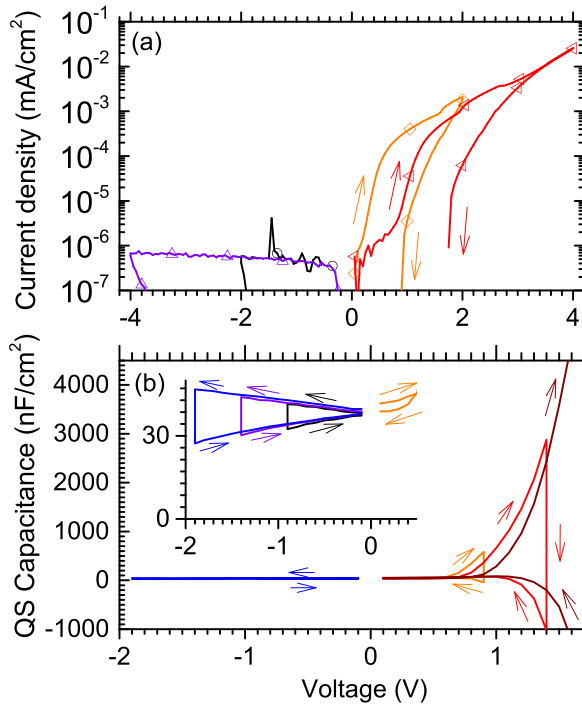


FIG. 2. (a) J - V characteristics of a pristine Al/LiF (30 nm)/poly(spirofluorene) (80 nm)/Ba/Al diode during subsequent cyclic voltage sweeps (0 V \rightarrow V_{\max} \rightarrow 0 V) where the maximum voltage V_{\max} is raised in steps of 2 V. (b) Quasi-static capacitance per unit area of an Al/LiF (30 nm)/poly(spirofluorene)/Ba/Al diode during subsequent cyclic voltage sweeps (0 V \rightarrow V_{\max} \rightarrow 0 V). Integration time: 4 s. The inset shows the capacitance region around the expected geometrical capacitance of the complete bilayer dielectric (30 nF/cm²).

When stepping the bias over the negative range, the quasi static capacitance is around 35 nF/cm², consistent with the geometrical capacitance $C_{\text{geo}} = (C_{\text{LiF}}^{-1} + C_{\text{polymer}}^{-1})^{-1}$ of 30 nF/cm² as expected for a bilayer dielectric composed of 30 nm LiF ($\epsilon_r = 9$ ²¹) and 80 nm of poly(spirofluorene) polymer ($\epsilon_r = 3$ (Refs. 22 and 23)). When scanning the bias over the positive range from 0 to +0.5 V, the capacitance measured is still close to the geometrical capacitance $C_{\text{geo}} \sim 30$ nF/cm², indicating that no charge is injected or extracted from the dielectric. When the bias exceeds +0.6 V, the capacitance measured exceeds C_{geo} in the part of the cyclic scan with $dV/dt > 0$. In the return part of the voltage sweep, with $dV/dt < 0$, C_{geo} is recovered. This behavior is consistent with injection of electrons into the organic semiconductor and trapping of the electrons at the LiF/polymer interface.¹⁸

To further characterize the electrical transport in the Al/LiF/poly(spirofluorene)/Ba/Al diodes, we have employed small-signal impedance measurements. The changes occurring in the frequency-dependence of the admittance as function of the applied dc bias is shown in Fig. 3(a). For zero applied dc bias, the parallel capacitance of the diodes, C_p , has a magnitude 30.4 nF/cm², which equals the total geometrical capacitance. At zero dc bias, the loss is negligible at all frequencies. This indicates that at zero bias, no charge carriers are injected or transported. Upon increasing the dc bias, both the capacitance and the loss at low frequency start to rise. The frequency response of the admittance shows that the device undergoes a change from a pure, capacitor-like behavior into a double-layer structure behavior. This is

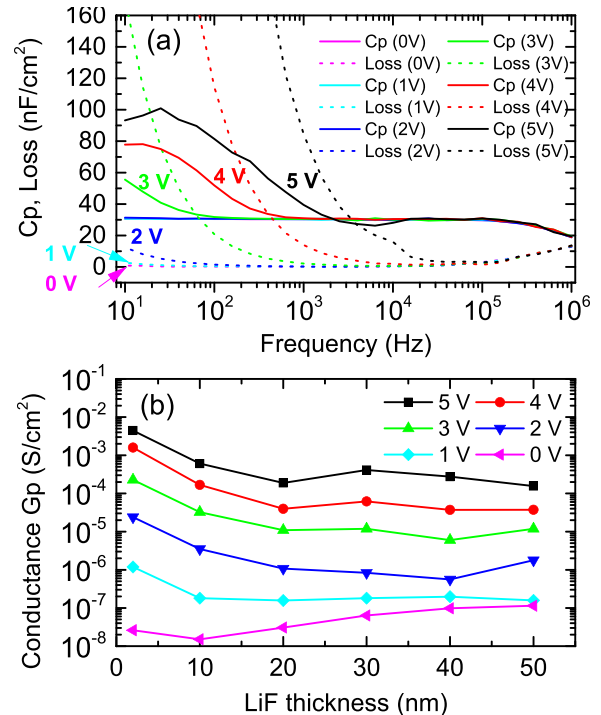


FIG. 3. (a) Small-signal impedance of an Al/LiF (30 nm)/poly(spirofluorene)/Ba/Al diode. The parallel capacitance per unit area (C_p) and Loss (dashed lines) are plotted as a function of the frequency for different dc bias voltages. (b) Parallel conductance per unit area (G_p) of Al/LiF/poly(spirofluorene)/Ba/Al diodes as a function of the thickness of the LiF layer, measured at an ac frequency of 10 Hz applying dc bias voltages in the range of 0 to +5 V.

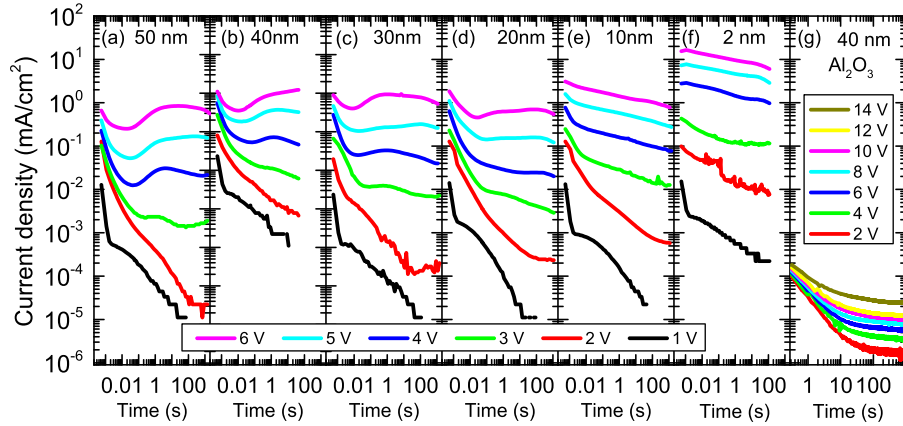


FIG. 4. Current density as a function of time for metal/insulator/poly(spirofluorene)/metal diodes in pristine state with LiF or Al_2O_3 as ionic semiconductor and insulator respectively. The thickness of the LiF layer is varied (a) 50 nm, (b) 40 nm, (c) 30 nm, (d) 20 nm, (e) 10 nm, and (f) 2 nm under positive bias voltage that is stepped from 0 V for $t < 0$ to constant positive voltage for $t > 0$, ranging from +1 V to +6 V. (g) The diode with 40 nm Al_2O_3 is subjected to bias voltage steps from +2 to +14 V.

because under bias the carrier injection causes a significant reduction in the polymer resistance. The corresponding polymer capacitance is effectively short-circuited and the high capacitive LiF layer starts to contribute to the device capacitance at low frequency. The capacitance shows a dispersion moving to higher frequency with increasing bias. This behavior is an indication that electrons accumulate at the halide interface layer.^{18,24} At high frequency the geometric capacitance is retained.

The ac transport characteristics have been determined as a function of the LiF layer thickness and are presented in Fig. 3(b). The capacitance at -5 V bias varies with the LiF thickness as expected for a bilayer dielectric (see supplementary material) and the conductance at zero bias is small. These observations confirm the integrity of the LiF layer and the absence of metallic shorts. Upon increasing the bias, the parallel conductance of the diodes, G_p , increases. Surprisingly, at low frequency (10 Hz) and at high bias (+5 V), the parallel conductance G_p of the diodes varies only very little with the thickness of the alkali halide layer (see Fig. 3(b)). While naively one might expect an exponential decrease of the conductance with thickness, the experiments show that for thicknesses above 10 nm, the ac conductances are essentially independent of the thickness of the LiF layer.

To further investigate the remarkable thickness dependence, we have performed time-dependent current measurements. This method is sensitive to the slow accumulation of charges as suggested by the quasi-static and low frequency capacitance measurements (Figs. 2(b) and 3(a)). The time evolution of the current density through the diode induced by a voltage step is presented in Fig. 4. The height of the voltage step (+1 to +6 V) and the thickness of the LiF layer in the diodes (2 to 50 nm) are varied systematically. For comparison we also provide current densities for diodes with similar structure but with Al_2O_3 as an inorganic dielectric (Fig. 4(g)).

For small voltage steps (1–2 V), we observe a transient current density that decays with time with very low current densities as asymptotic limit. This behavior is also observed for the Al_2O_3 /polymer diodes. The transient current is independent of the LiF thickness and due to *charging* of trap states at the insulator/poly(spirofluorene) interface by electrons injected via the Ba/Al top electrode (see Fig. 1(c)).

However, the current density measured immediately after a large bias voltage step, J_{ini} , is inversely proportional to the thickness of the LiF layer (see Fig. 5). At high bias, the polymer is effectively short-circuited and the current is due to the displacement current expected for polarizing an insulating LiF layer by accumulation of electrons at the LiF/polymer interface. A quantitative interpretation is presented in more detail in Sec. 4 of the supplementary material.

Interestingly, for diodes with LiF layer exceeding 10 nm in thickness and bias voltages $\geq +4$ V, we notice that the initial decay of the current density due to charging and polarization is followed by an *increase* in current density over time at times $t > 1$ s. This increase is most clearly visible in the data for the 50 nm thick film (Fig. 4(a)) and is not observed for Al_2O_3 /polymer diodes (Fig. 4(g)). The increase in current density in the LiF diodes does not persist indefinitely: eventually the current density reaches a quasi-steady state level that increases with increasing applied bias. We note that the current transients are fully reversible, provided that in between the measurements the diode is exposed to light from a fluorescent light tube for 10 min, in order to optically detrapp all accumulated charge carriers,²⁵ or left to equilibrate for at least several hours. Experiments on

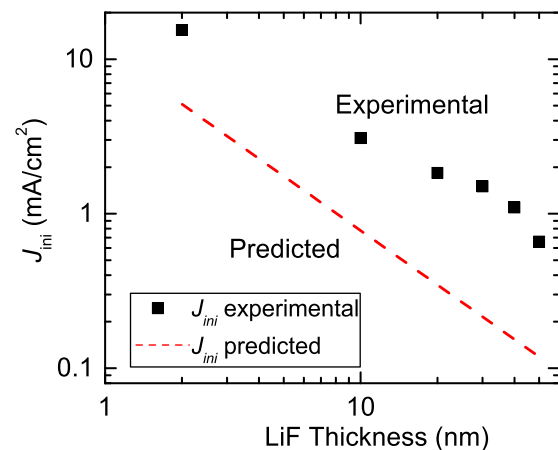


FIG. 5. Initial current densities J_{ini} for the Al/LiF/poly(spirofluorene)/Ba/Al diodes of Fig. 4, recorded at 0.56 ms after stepping the bias voltage from 0 to +5 V. Black squares: experimental data from Fig. 4, dashed line, prediction based on the bias dependent electron current in the semiconductor and the geometric capacitance of the pristine LiF layer (see Ref. 25 and Eq. (S8) in supplementary material).

LiF/polymer diodes at reduced temperature indicate that the time interval between the onset of bias application and the moment at which the current density through the diode reaches its minimum becomes larger at lower temperatures. Also the magnitude of the saturation current density is reduced at lower temperature. The temperature dependence indicates that the current is partially controlled by hopping transport in the poly(spirofluorene) layer.

Further insight into the remarkable current transients for the metal/LiF/polymer/metal diodes can be obtained by plotting the saturation level of the current density as a function of the applied stepped bias voltage (see Fig. 6). The steady state saturation current, J_{sat} , we define as the current density reached 100 s after application of the bias voltage step to the diode as shown in Fig. 4. The saturation current densities for diodes with LiF layers exceeding 10 nm in thickness are found to be very similar. At bias voltages $\geq +3$ V, the current density through the LiF/polymer diodes is virtually *independent* of the thickness of the LiF layer (see Fig. 6), which confirms the independence of the parallel conductance G_p of LiF thickness as obtained from the impedance measurements under constant dc bias (Fig. 3(b)).

We note that Fig. 6(a) also shows the current density in an electron-only diode with an Al/poly(spirofluorene)/Ba/Al structure. The current density shows a $J \propto V^{6.5}$ dependence on voltage, which is consistent with earlier measurements on electron-only current in poly(spirofluorene) diodes and characteristic for trap limited charge transport.¹² The current

density in the LiF diodes, however, is significantly lower than the current in the electron-only diode, which indicates the presence of an additional barrier.

As shown in Fig. 6(a), to estimate the potential over the barrier, $V_{barrier}$, we take the simplifying assumption that the potential difference over the poly(spirofluorene) layer required for transport of electrons with a specific current density in a LiF/polymer diode, equals the potential difference needed to sustain a same current density in the electron-only diode. The potential drop over the bulk LiF layer can be disregarded as the current density in the LiF diodes does not depend on LiF thickness. The current density can then be presented as a function of $V_{barrier}$. As shown by the solid black line in Fig. 6(b), the transport could be described by Fowler-Nordheim tunneling, yielding a barrier of about 1 nm.²³ The use of Simmons's relation for the tunneling current,²⁶ gives a similar estimate for the effective width of the barrier. The barrier might be at the polymer/LiF interface.

In summary, the charge transport through the combined alkali halide/polymer layer is attributed to electrons. Electron transport through the polymer occurs via hopping type motion and is trap limited. Alkali halides are known to exhibit high electron mobilities but poor hole transport.^{27,28} In principle also ionic conductivity in the alkali halide layer might contribute to the ac transport. However, the strong dependence of the loss on dc bias and the absence of any significant loss under reverse bias conditions rule out a significant contribution of bulk ionic conductivity to the ac admittance. Because the polymer does not support ionic transport, also no direct contribution of ion motion to the (quasi-)dc characteristics is expected.

IV. ELECTRO-OPTICAL CHARACTERIZATION

In order to account for the surprisingly efficient transport of electrons through the relatively thick LiF layers, we now propose that positively charged defects accumulate in the LiF layer and assist in the tunneling of electrons across the potential barrier at the LiF/polymer interface. Direct experimental evidence for accumulation of charged defects is obtained from electro-optical reflection measurements on ITO/LiF/poly(spirofluorene)/Ba/Al diodes where a transparent bottom ITO contact is employed for optical access to the active layers. The Ba/Al top contact is highly reflective, allowing for measurements of the specular reflection on the complete diodes at small angles of incidence as a function of wavelength. In the visible and NIR spectral ranges, the polymeric semiconductor is transparent so that one can probe for sub-gap optical transitions associated with defects induced by the application of bias voltage stress.

Fig. 7(a) shows the relative differential change in reflection of light ($-\Delta R/R$) as a function of photon energy induced by application of +15 V bias. Only a positive bias voltage results in a reduction of the reflectivity; a negative bias voltage gives no significant change. We notice in the differential reflectance a broad band centered around 700 nm. We attribute this band to sub-band gap absorption in the LiF layer induced by the bias stress. The spectrum does not show any

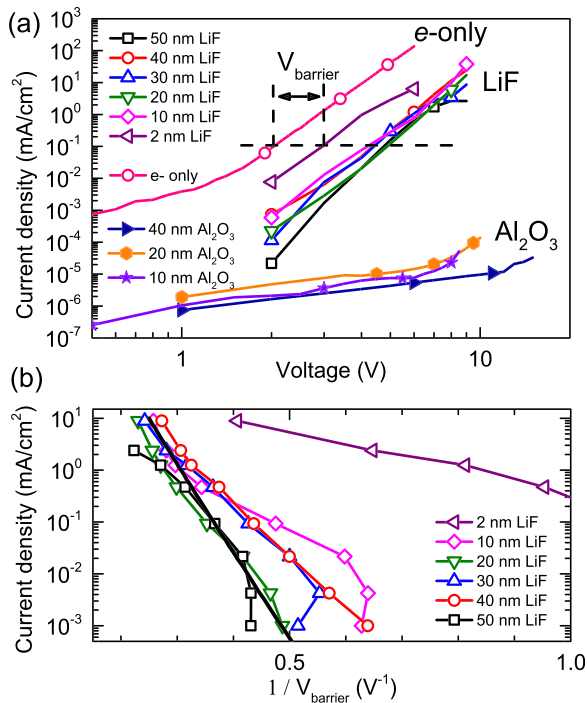


FIG. 6. (a) J - V characteristics of an electron-only diode and saturation current, J_{sat} , of diodes incorporating LiF and Al_2O_3 interlayers with thicknesses from 2 to 50 nm. (b) Difference in the applied voltage, $V_{barrier}$, needed to maintain the same current density in an Al/poly(spirofluorene)(80 nm)/Ba/Al electron-only diode and in an Al/LiF/poly(spirofluorene)(80 nm)/Ba/Al diode as extracted from Fig. 4. The thickness of the LiF is varied from 2 to 50 nm. Black solid line prediction for the Fowler-Nordheim tunneling current using a barrier of about 1 nm.²³

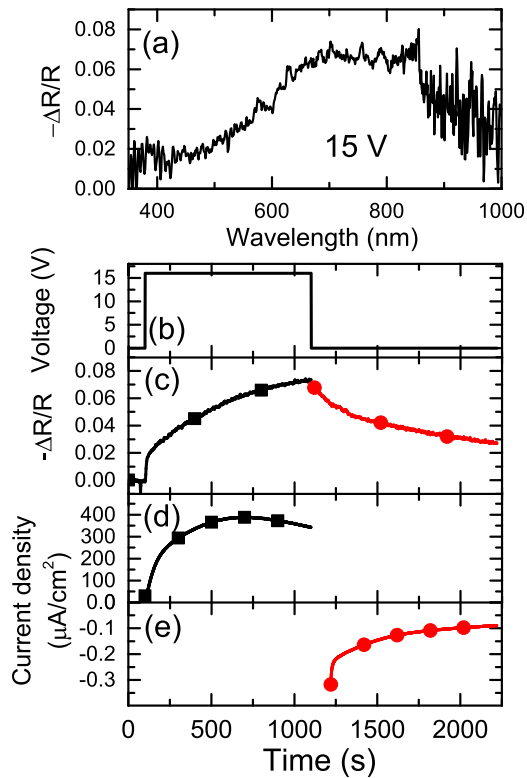


FIG. 7. (a) Relative change in reflectivity ($-\Delta R/R$) for a ITO/LiF(100 nm)/poly(spirofluorene)(80 nm)/Ba/Al diode as a function of wavelength. (b-e) Time dependence of $-\Delta R/R$ probed at a wavelength of 800 nm induced a bias voltage step from 0 to +15 V as shown in (b). (d) Positive part of the transient current density measured simultaneously with the change in reflectivity (c) indicating charging. (e) Negative part of the current density indicating discharging.

significant bleaching of the absorption band of the neutral poly(spirofluorene) absorption band below 400 nm. This indicates that the induced absorption is not due to negatively charged polarons in the polymer. The position of the band may be tentatively assigned to absorption by two adjacent anion vacancies in the LiF accommodating a single electron, *i.e.*, an F_2^+ defect center. This defect center can also be observed in bulk LiF crystals with radiation defects.^{29,30}

Upon application of a stepped bias voltage (Fig. 7(b)) going from zero to 15 V, we have monitored the temporal intensity of the defect band (see Fig. 7(c)). The intensity increases slowly with time indicating a slow built-up of the defects. Importantly, upon removing the applied bias, the reflectivity reverts spontaneously and slowly approaches its original level, see Fig. 7(c). The recovery can be accelerated by application of reverse bias.

By measuring the current density through the diode simultaneously with the change in reflectivity during the bias stress and subsequent recovery, we can correlate the changes in optical properties to the building up of charge density in the diode (Figs. 7(d) and 7(e)). During recovery under short circuit conditions, we observe a spontaneous discharging current with sign opposite to that of the current during bias voltage stress. The decay of the discharging current takes place on the same timescale as the decay of the differential reflectivity, compare Figs. 7(c) and 7(e). We note that application of a reverse bias does not to introduce the charged defect in

the LiF. Furthermore, diodes incorporating a 30 nm Al_2O_3 layer instead of LiF, do not show any appreciable change in reflection of light in the wavelength range from 350 to 2000 nm. No defects are formed in Al_2O_3 ; it behaves as a normal dielectric.

Upon integrating the discharge transient we find that the areal number density of elementary charges is $3 \times 10^{19} m^{-2}$. This number is two orders of magnitude larger than the polarization surface charge density expected for a 100 nm LiF thick dielectric at a bias of +15 V. This indicates that besides electrons at the LiF/polymer interface, trapped positive charges must be present inside the LiF layer. Considering also the thickness of the LiF layer (100 nm), it follows from the areal density listed above that the bulk of the LiF layer is doped with a maximum local number density of positive charges equal to or exceeding $10^{25} m^{-3}$ at +15 V. These high doping levels explain why the current density in the LiF/poly(spirofluorene) diodes is independent of the LiF layer thickness.

V. DISCUSSION AND CONCLUSION

In summary, our experimental data indicate that under prolonged bias voltage stress of Al/LiF/poly(spirofluorene)/Ba/Al diodes first electrons are accumulated at the polymer side of LiF/poly(spirofluorene) interface. With time under bias stress, the positive charge builds up in the LiF layer. The layer gets bulk doped with a charge density exceeding $10^{25} m^{-3}$, presumably with charged Frenkel F_2^+ defect centers. The built-up of charge at the inorganic/organic semiconductor internal interface promotes band-to-band tunneling of electrons from the lowest unoccupied level in the polymer into the conduction band of the LiF.²³ The doped LiF layers are highly conductive, which explains that the current density in the diodes is independent of the LiF layer thickness.

The doping of the relatively thick LiF layers is not permanent when the bias voltage does not exceed the band gap of LiF. The charged double layer at the LiF/polymer interface is metastable for LiF layers exceeding 10 nm in thickness and the double layer decays on a timescale exceeding seconds. The diode returns to its pristine state upon exposure to UV light in order to optically detrap the accumulated charge carriers or when the diode is left to equilibrate for a few hours. The recovery can be accelerated by applying a reverse bias.

The accumulation of the positive defects depends on the nature of the inorganic semiconductor and occurs to a much lesser extent in Al_2O_3 /polymer diodes. This is evidenced by the lower tunneling current densities in the Al_2O_3 diodes and the absence of any detectable optical signal from defects in this insulator. These variations in the defect generation for the oxide and halide insulators are in line with earlier research showing differences between electroforming of Al_2O_3 which is predominantly field driven³¹ and in LiF where the electroforming is voltage driven.³² The accumulation of positive charge in the LiF represents a first, reversible stage in the electroforming process for bias voltages below the bandgap.

Our conclusion that injection of electrons from the semi-conducting polymer into LiF is made possible by the presence of charge defects is supported by previous research on metal-insulator-metal (MIM) structures with only alkali halide as insulator. Based on photoconductivity measurements on additively colored alkali halide crystals, Von Hippel *et al.* argued that field emission from a metal electrode into the alkali halide is possible due to built-up of space charge in the alkali halide as the result of ionization of the chemically induced color centers.^{33–35}

Electrically induced defect formation in alkali halide MIM diodes is well known from extensive studies on dielectric breakdown in these structures. Breakdown in alkali halide results in filamentous conduction, exhibiting voltage controlled negative differential resistance and memory effects^{36,37} similar to the alkalihalide/polymer MIM diodes studied here.³⁸ The critical field strength for alkali halide MIM diodes corresponding to breakdown increases with decreasing alkalihalide thickness^{39,40} and it has been suggested that a specific voltage threshold exists for electroforming that scales with the bandgap of the alkalihalide.⁴¹ Similarly in alkalihalide/polymer diodes, the electroforming voltage also scales with the bandgap of the alkalihalide. A major difference between alkalihalide and alkalihalide/polymer diodes is, however, that in the case of just alkali halide insulating layers, there is no evidence for reversible enhancement of electrical conduction prior to breakdown.⁴² Thus a major variation in the electrical behavior of MIM diodes with only LiF and with LiF/semiconducting polymer as insulator seems to be that in the case of the LiF/polymer diodes, the defects required for reversible pre-breakdown conduction can be induced electrically without causing immediate breakdown. We attribute this to the presence of the alkali halide/polymer interface.

In conclusion, the efficient transport of electrons through thick LiF layers in the early stage of electroforming of LiF/semiconducting polymer MIM diodes observed here is attributed to electrically induced defects in the alkali halide. The electron transport is consistent with the selectivity for electrons of thin LiF charge injection layers commonly used in organic light emitting diodes and solar cells. The operation of light emitting diodes with thin LiF electron injection layer at the cathode, suggests that for thin layers, the electroforming of the LiF can be arrested in the early stage, at least temporarily.

ACKNOWLEDGMENTS

We thank Dr. M. Kuik for help with the fabrication and characterization of the electron-only diode. The work forms part of the research programme of the Dutch Polymer Institute (DPI), project DPI #704, BISTABLE. We gratefully acknowledge the financial support received from Fundação para Ciência e Tecnologia (FCT) through the research Instituto de Telecomunicações (IT-Lx), the project Memristor based Adaptive Neuronal Networks (MemBrAiNN), PTDC/CTM-NAN/122868/2010, and funding by KAU from project 71-100-35-HiCi, from the European Community Seventh Framework Programme FP7/2007-2013 project 212311, ONE-P and from the Dutch

Ministry of Education, Culture and Science (Gravity program 024.001.035).

- ¹D. B. Sirdeshmukh, L. Sirdeshmukh, and K. G. Subhadra, *Alkali Halides: A Handbook of Physical Properties* (Springer Verlag, 2001).
- ²D. A. Lapiano-Smith, E. A. Eklund, F. J. Himpsel, and L. J. Terminello, *Appl. Phys. Lett.* **59**, 2174 (1991).
- ³L. S. Hung, C. W. Tang, and M. G. Mason, *Appl. Phys. Lett.* **70**, 152 (1997).
- ⁴G. E. Jabbour, Y. Kawabe, S. E. Shaheen, J. F. Wang, M. M. Morrell, and B. Kippelen, *Appl. Phys. Lett.* **71**, 1762 (1997).
- ⁵C. J. Brabec, S. E. Shaheen, C. Winder, N. S. Sariciftci, and P. Denk, *Appl. Phys. Lett.* **80**, 1288 (2002).
- ⁶S. E. Shaheen, G. E. Jabbour, M. M. Morrell, Y. Kawabe, B. Kippelen, N. Peyghambarian, M. F. Nabor, R. Schlaf, E. A. Mash, and N. R. Armstrong, *J. Appl. Phys.* **84**, 2324 (1998).
- ⁷T. M. Brown, R. H. Friend, I. S. Millard, D. J. Lacey, J. H. Burroughes, and F. Cacialli, *Appl. Phys. Lett.* **79**, 174 (2001).
- ⁸T. M. Brown, R. H. Friend, I. S. Millard, D. J. Lacey, T. Butler, J. H. Burroughes, and F. Cacialli, *J. Appl. Phys.* **93**, 6159 (2003).
- ⁹M. G. Mason, C. W. Tang, L.-S. Hung, P. Raychaudhuri, J. Madathil, D. J. Giesen, L. Yan, Q. T. Le, Y. Gao, S.-T. Lee, L. S. Liao, L. F. Cheng, W. R. Salaneck, D. A. dos Santos, and J. L. Brédas, *J. Appl. Phys.* **89**, 2756 (2001).
- ¹⁰Y. D. Jin, X. B. Ding, J. Reynaert, V. I. Arkhipov, G. Borghs, P. L. Heremans, and M. Van der Auweraer, *Org. Electron.* **5**, 271–281 (2004).
- ¹¹R. T. Poole, J. G. Jenkin, J. Liesegang, and R. C. G. Leckey, *Phys. Rev. B* **11**, 5179 (1975).
- ¹²H. T. Nicolai, A. Hof, J. L. M. Oosthoek, and P. W. M. Blom, *Adv. Funct. Mater.* **21**, 1505–1510 (2011).
- ¹³P. A. Cox and A. A. Williams, *Surf. Sci.* **175**, L782–L786 (1986).
- ¹⁴K. S. Song and R. T. Williams, *Self Trapped Excitons*, 2nd ed. (Springer Verlag, 1996).
- ¹⁵A. Lushchik, C. Lushchik, V. Nagirnyi, S. Pazyzbek, O. Sidletskiy, K. Schwartz, E. Shablonin, A. Shugai, and E. Vasil'chenko, *Phys. Status Solidi B* **250**, 261–270 (2013).
- ¹⁶Q. Chen, H. L. Gomes, P. R. F. Rocha, D. M. de Leeuw, and S. C. J. Meskers, *Appl. Phys. Lett.* **102**, 153509 (2013).
- ¹⁷J. Hutchby and M. Garner, Assessment of the Potential and Maturity of Selected Emerging Research Memory Technologies, <http://www.itrs.net/Links/2013ITRS/2013Chapters/2013ERD.pdf>.
- ¹⁸B. F. Bory, S. C. J. Meskers, R. A. J. Janssen, H. L. Gomes, and D. M. de Leeuw, *Appl. Phys. Lett.* **97**, 222106 (2010).
- ¹⁹T. J. Mege, *Rev. Sci. Instrum.* **57**, 2798 (1986).
- ²⁰K. Ziegler and E. Klausmann, *Appl. Phys. Lett.* **26**, 400 (1975).
- ²¹R. P. Lowndes and D. H. Martin, *Proc. R. Soc. London A* **308**, 473–496 (1969).
- ²²S. L. M. van Mensfoort, S. I. E. Vulto, R. A. J. Janssen, and R. Coehoorn, *Phys. Rev. B* **78**, 085208 (2008).
- ²³See supplementary material at <http://dx.doi.org/10.1063/1.4917461> for thickness characterization, electrical characteristics at reduced temperature, modeling of tunneling transport through the alkali halide / organic semiconductor interface, modeling of the time-dependence of the current density, further optoelectronic characterization of charge accumulation and admittance spectroscopy.
- ²⁴H. L. Gomes, A. R. V. Benvenho, D. M. de Leeuw, M. Cölle, P. Stallinga, F. Verbakel, and D. M. Taylor, *Org. Electron.* **9**, 119–128 (2008).
- ²⁵Q. Chen, B. F. Bory, A. Kiazadeh, P. R. F. Rocha, H. L. Gomes, F. Verbakel, D. M. De Leeuw, and S. C. J. Meskers, *Appl. Phys. Lett.* **99**, 083305 (2011).
- ²⁶J. G. Simmons, *J. Appl. Phys.* **34**, 2581–2590 (1963).
- ²⁷R. K. Ahrenkiel and F. C. Brown, *Phys. Rev.* **136**, A223 (1964).
- ²⁸C. H. Seager and D. Emin, *Phys. Rev. B* **2**, 3421 (1970).
- ²⁹G. Baldacchini, *J. Lumin.* **100**, 333–343 (2002).
- ³⁰G. Baldacchini, S. Bollanti, F. Bonfigli, P. Di Lazzaro, A. Ya. Faenov, F. Flora, T. Marolo, R. M. Montecali, D. Murra, E. Nichelatti, T. Pikuz, A. Reale, L. Reale, A. Ritucci, and G. Tomassetti, *IEEE J. Quant. Electron.* **10**, 1435–1445 (2004).
- ³¹F. Verbakel, S. C. J. Meskers, R. A. J. Janssen, H. L. Gomes, M. Cölle, M. Büchel, and D. M. de Leeuw, *Appl. Phys. Lett.* **91**, 192103 (2007).
- ³²B. F. Bory, J. Wang, H. L. Gomes, R. A. J. Janssen, D. M. De Leeuw, and S. C. J. Meskers, *Appl. Phys. Lett.* **105**, 233502 (2014).

- ³³A. von Hippel, E. P. Gross, J. G. Jelatis, and M. Geller, *Phys. Rev.* **91**, 568 (1953).
- ³⁴M. Geller, *Phys. Rev.* **101**, 1685 (1956).
- ³⁵R. Williams, *J. Phys. Chem. Solids* **25**, 853 (1964).
- ³⁶H. Biederman, *Thin Solid Films* **18**, 39–43 (1973).
- ³⁷H. Biederman, *Vacuum* **26**, 513 (1976).
- ³⁸B. F. Bory, P. R. F. Rocha, R. A. J. Janssen, H. L. Gomes, D. M. De Leeuw, and S. C. J. Meskers, *Appl. Phys. Lett.* **105**, 123302 (2014).
- ³⁹C. Weaver and J. E. S. Macleod, *Br. J. Appl. Phys.* **16**, 441 (1965).
- ⁴⁰K. W. Plessner, *Proc. Phys. Soc.* **60**, 243 (1948).
- ⁴¹A. K. Vijh, *J. Mater. Sci.* **9**, 853 (1974).
- ⁴²J. L. Smith and P. D. Budenstein, *J. Appl. Phys.* **40**, 3491 (1969).